

## Yi-Cheng Wu

Engineer  
Mechanical System Research Laboratory,  
Industrial Technology Research Institute,  
Hsinchu 31040, Taiwan  
e-mail: easonwu@gmail.com

## Kuan-Yu Chen

Ph.D. Candidate  
Department of Mechanical Engineering,  
National Chiao Tung University,  
Hsinchu 30010, Taiwan  
e-mail: cky.me92g@nctu.edu.tw

## Chung-Biau Tsay<sup>1</sup>

Chair Professor  
Department of Mechanical Engineering,  
Minghsin University of Science and Technology,  
Hsinfong, Hsinchu 30401, Taiwan  
e-mail: cbtsay@mail.nctu.edu.tw

## Yukinori Ariga

Professor  
Department of Mechanical Engineering,  
Nippon Institute of Technology,  
Saitama 345-8501, Japan  
e-mail: ariga@nit.ac.jp

# Contact Characteristics of Circular-Arc Curvilinear Tooth Gear Drives

*In this paper, the circular-arc curvilinear tooth gear drive is proposed. The gear and pinion tooth surfaces are generated by two complemented circular-arc rack cutters with curvilinear tooth-traces. According to the theory of gearing, the mathematical model of the proposed gear is developed. The tooth contact analysis technique is utilized to investigate the kinematical errors of circular-arc curvilinear tooth gear drives under different assembly errors. Contact patterns of the circular-arc curvilinear tooth gear drive are simulated by the developed computer-aided tooth contact analysis programs and surface topology method. Numerical examples are presented to show the kinematical errors of the circular-arc curvilinear tooth gear set under different assembly conditions. Relations among the circular-arc tooth profile, curvilinear tooth-trace, contact ratio, contact pattern, and kinematical error are also demonstrated by numerical examples.*

[DOI: 10.1115/1.3151805]

*Keywords:* mathematical model, kinematical error, curvilinear gear, circular-arc tooth profile, contact ratio, contact pattern

## 1 Introduction

It is known that gears are widely used in industry for power transmissions because of their high efficiencies. Liu [1] investigated the characteristics of curvilinear gears and proposed the manufacture method by applying a face-mill cutter to generate curvilinear gears in 1988. The merits of curvilinear gears are higher bending strength, lower noise, better lubrication effect, no axial thrust force, avoiding edge contact, etc. [1]. In 2000, Tseng and Tsay [2] developed a mathematical model of cylindrical gears with curvilinear shaped teeth generated by using an imaginary rack cutter with straight-edged tooth profiles and investigated the tooth undercutting of curvilinear gears. However, in practical manufacturing, gears are usually cut by a hobbing machine. Therefore, Tseng and Tsay [3] proposed a generating process of using a straight-edged hob cutter to generate the curvilinear gear. A helical gear with circular tooth profiles was proposed by Wildhaber [4] in 1926 and Novikov [5] in 1956. This type of gears became popular in 1960s because of their low contact stresses. Litvin and Tsay [6] investigated the mathematical model and tooth contact analysis of circular-arc helical gears by considering the pinion and gear were generated by two imaginary circular-arc rack cutters.

In this paper, a curvilinear tooth-trace gear pair with circular-arc tooth profiles is proposed. The generation mechanism of the proposed gear drive can be accomplished by considering two complemented rack cutters with circular-arc tooth profiles and curvilinear tooth-traces to generate the gear and pinion. The gear pair with a curvilinear tooth-trace results in a crowning effect on the tooth width direction. Therefore, the bearing contact is localized and located at the middle section of the tooth width, and the

proposed circular-arc curvilinear tooth gear pair is theoretically in point contact. Thus, the proposed gear drive allows axial alignments and has no axial thrust force. Due to elasticity of tooth surfaces, the instantaneous contact point is spread over an elliptical area. A larger curvature of the circular-arc tooth profiles of the proposed curvilinear gear drive can increase the length of minor axis of the contact ellipse, and a smaller curvature of the curvilinear tooth-trace can increase the length of major axis of the contact ellipse. Therefore, if the curvatures of two mating gear tooth surfaces were properly designed, the circular-arc curvilinear tooth gear drive is a kind of gears with a higher loading capacity, and it operates without axial thrust force. The mathematical model of the curvilinear gear with circular-arc tooth profiles is developed according to the gear theory [7,8] and the proposed gear generation mechanism. The tooth contact analysis (TCA) simulation of the circular-arc curvilinear tooth gear drive can be performed according to the established mathematical model.

The TCA has been utilized herein to investigate the kinematical error (KE) of the circular-arc curvilinear tooth gear drive meshing under ideal and error assembly conditions. The location and shape of contact ellipses of the mating gear and pinion can be also simulated by applying the TCA results and surface topology method [9]. Six examples are presented to show the relations among the radius of circular-arc tooth profile, radius of curvilinear tooth-trace, contact ratio, contact pattern, and KE of the gear pair under different assembly conditions.

## 2 Mathematical Model of the Circular-Arc Curvilinear Tooth Gear

Figure 1 illustrates the generating mechanism, proposed by Liu [1] for cutting of curvilinear gears, where axis *A-A* represents the rotation axis of the gear blank, and axis *B-B* expresses the cutter spindle. The spindle of the face-mill cutter with radius  $R_{ab}$  rotates about the axis *B-B* with an angular velocity  $\omega_c$  and translates with a linear velocity  $\omega_1 r_1$  to the right, where  $r_1$  is the pitch radius of

<sup>1</sup>Corresponding author.

Contributed by the Power Transmission and Gearing Committee of ASME for publication in the JOURNAL OF MECHANICAL DESIGN. Manuscript received August 2, 2007; final manuscript received April 7, 2009; published online July 9, 2009. Review conducted by Avinash Singh.

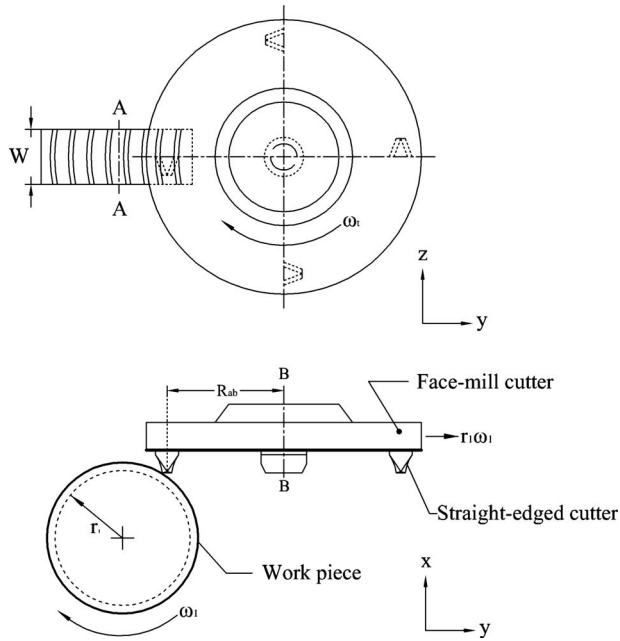


Fig. 1 Generating mechanism for curvilinear gears

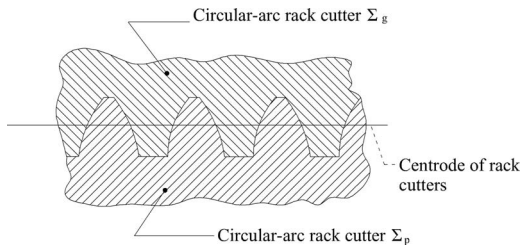


Fig. 2 Normal cross section of the proposed circular-arc rack cutters

the gear blank and  $\omega_1$  is the angular velocity of it. The work piece is indexed to one tooth and the generating cycle is repeated until all the gear teeth and spaces are produced.

Although the gear is generated by a face-mill cutter, however, it can also be considered that the gear is generated by a rack cutter. In this paper, the circular-arc curvilinear tooth gear pair is generated by two complemented rack cutters  $\Sigma_p$  and  $\Sigma_g$ . The normal sections of the rack cutters  $\Sigma_p$  and  $\Sigma_g$  are shown in Fig. 2. The enlarged normal section of the circular-arc rack cutter  $\Sigma_g$  and its corresponding design parameters are shown in Fig. 3. Coordinate

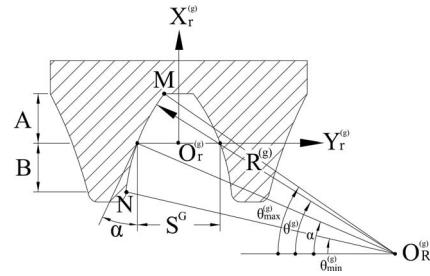


Fig. 3 Normal cross section of the circular-arc rack cutter  $\Sigma_g$

system  $S_r^{(g)}(X_r^{(g)}, Y_r^{(g)}, Z_r^{(g)})$  is rigidly attached to the middle of transverse section of the imaginary rack cutter. Figure 4 illustrates the relations between rack cutter coordinate system  $S_c^{(g)}(X_c^{(g)}, Y_c^{(g)}, Z_c^{(g)})$  and rack cutter normal cross section coordinate system  $S_r^{(g)}$ . The surface equation of the imaginary rack cutter surface  $\Sigma_g$  and its unit normal vector can be expressed in coordinate system  $S_c^{(g)}(X_c^{(g)}, Y_c^{(g)}, Z_c^{(g)})$  as follows:

$$\begin{aligned} \mathbf{R}_c^{(g)} &= \begin{bmatrix} x_c^{(g)} \\ y_c^{(g)} \\ z_c^{(g)} \end{bmatrix} \\ &= \begin{bmatrix} -R^{(g)}(\sin \alpha - \sin \theta^{(g)}) \\ R_{ab}(1 - \cos \gamma^{(g)} \pm \cos \gamma^{(g)} \left( -\frac{S^G}{2} + R^{(g)}(\cos \alpha - \cos \theta^{(g)}) \right)) \\ \sin \gamma^{(g)} \left( R_{ab} \pm \left( \frac{S^G}{2} - R^{(g)}(\cos \alpha - \cos \theta^{(g)}) \right) \right) \end{bmatrix} \end{aligned} \quad (1)$$

where

$$-\sin^{-1} \left[ \frac{W}{2R_{ab}} \right] \leq \gamma^{(g)} \leq \sin^{-1} \left[ \frac{W}{2R_{ab}} \right] \quad (2)$$

and

$$\mathbf{n}_c^{(g)} = \begin{bmatrix} \mathbf{n}_{X_c}^{(g)} \\ \mathbf{n}_{Y_c}^{(g)} \\ \mathbf{n}_{Z_c}^{(g)} \end{bmatrix} = \begin{bmatrix} \sin \theta^{(g)} \\ \pm (-\cos \gamma^{(g)} \cos \theta^{(g)}) \\ \pm \sin \gamma^{(g)} \cos \theta^{(g)} \end{bmatrix} \quad (3)$$

where the upper sign of symbol “ $\pm$ ” indicates the right-side of the rack cutter surface,  $\theta^{(g)}$  is a design parameter of the circular-arc rack cutter ranging from  $\theta_{\min}^{(g)}$  to  $\theta_{\max}^{(g)}$ ,  $\gamma^{(g)}$  indicates the instant-

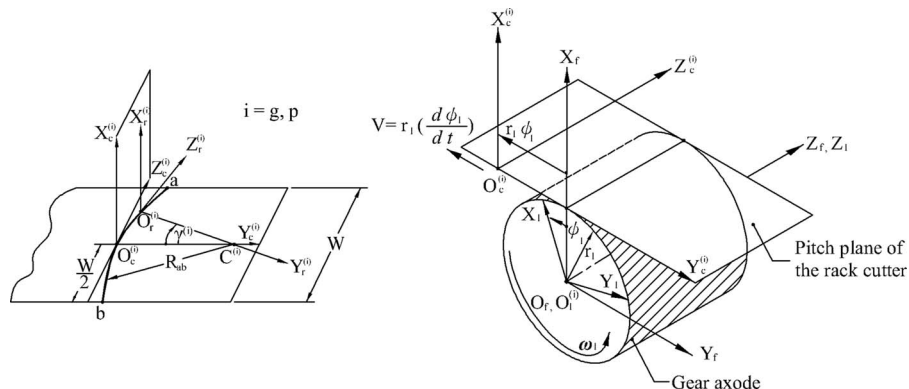


Fig. 4 Relationship among coordinate systems  $S_c^i$ ,  $S_r^i$ , and  $S_f$

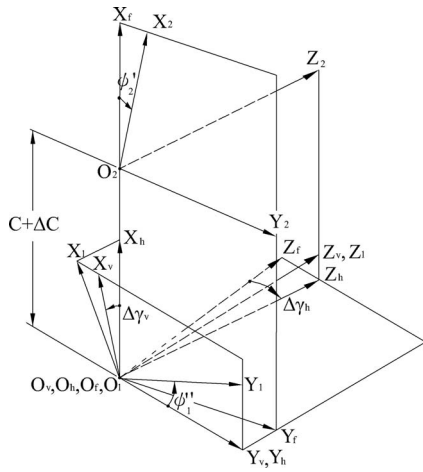


Fig. 5 Coordinate systems for simulation of a gear pair meshed with assembly errors

neous position of the rack cutter normal cross section  $S_r^{(g)}$ ,  $\alpha$  denotes the normal pressure angle,  $R^{(g)}$  represents the radius of the circular-arc  $\widehat{MN}$ ,  $R_{ab}$  denotes the radius of curvilinear tooth-trace, and  $W$  represents the tooth width of the curvilinear tooth gear.

In the generation process, the relative velocity of the gear with respect to the rack cutter,  $\mathbf{V}^{(12)}$ , is perpendicular to their common normal,  $\mathbf{n}$ . Therefore, the following equation must be observed:

$$\mathbf{n} \cdot \mathbf{V}^{(12)} = 0 \quad (4)$$

Equation (4) is the so called “meshing equation.” Based on the meshing equation, parameters  $\gamma^{(g)}$ ,  $\theta^{(g)}$ , and  $\phi_1$  can be expressed in the following implicit form:

$$f(\gamma^{(g)}, \theta^{(g)}, \phi_1) = -\frac{R^{(g)}}{4} (\mp 2R_{ab} - S^G + 2R^{(g)} \cos \alpha - 2R^{(g)} \cos \theta^{(g)})$$

$$\{2 \cos \gamma^{(g)} [r_1(-1 + \omega_1) \cos \theta^{(g)} + R^{(g)} \omega_1 \sin(\alpha - \theta^{(g)})]$$

$$+ \sin \theta^{(g)} [\mp 2R_{ab} \omega_1 \pm 2r_1 \phi_1 + (\pm 2R_{ab} + S^G) \omega_1 \cos \gamma^{(g)}] = 0 \quad (5)$$

and the locus of the rack cutter surfaces can be obtained by applying the following homogeneous coordinate transformation matrix equation:

$$\mathbf{R}_1^{(g)} = \mathbf{M}_{1c} \mathbf{R}_c^{(g)} = \begin{bmatrix} \cos \phi_1 & -\sin \phi_1 & 0 & r_1(\cos \phi_1 + \phi_1 \sin \phi_1) \\ \sin \phi_1 & \cos \phi_1 & 0 & r_1(\sin \phi_1 - \phi_1 \cos \phi_1) \\ 0 & 0 & 1 & 0 \\ 0 & 0 & 0 & 1 \end{bmatrix} \begin{bmatrix} x_c^{(g)} \\ y_c^{(g)} \\ z_c^{(g)} \\ 1 \end{bmatrix} \quad (6)$$

where symbol  $r_1$  denotes the radius of the gear pitch circle and  $\phi_1$  expresses the gear rotation angle during the gear generation process. The mathematical model of the circular-arc curvilinear tooth gear surfaces can be obtained by considering Eqs. (5) and (6), simultaneously. By applying the similar process, the mathematical model of the curvilinear pinion surfaces with circular-arc tooth profiles can also be derived.

### 3 Tooth Contact Analysis

**3.1 Analysis on Kinematical Errors.** The KE of a gear drive, induced due to assembly errors, is defined as the difference between the actual and ideal rotation angles of the output shaft with reference to the input shaft. The assembly errors of a gear drive can be simulated by changing the settings and orientations of coordinate systems  $S_v(X_v, Y_v, Z_v)$  and  $S_h(X_h, Y_h, Z_h)$ , as shown

in Fig. 5, where coordinate systems  $S_1(X_1, Y_1, Z_1)$  and  $S_2(X_2, Y_2, Z_2)$  are attached to the gear and pinion, respectively, in which axes  $Z_1$  and  $Z_2$  stand for the rotation-axes of the gear and pinion. Symbols  $\phi_1'$  and  $\phi_2'$  represent the actual rotation angles of the gear and pinion under assembly errors, respectively. Coordinate system  $S_f(X_f, Y_f, Z_f)$  is the fixed coordinate system, and coordinate systems  $S_v(X_v, Y_v, Z_v)$  and  $S_h(X_h, Y_h, Z_h)$  are setup for simulations of the horizontal misaligned angle  $\Delta\gamma_h$  and vertical misaligned angle  $\Delta\gamma_v$ .  $C$  is the ideal center distance of the gear pair, and  $\Delta C$  is the center distance assembly error. When applying the TCA method to calculate the KE of the circular-arc curvilinear tooth gear pair, the normal and position vectors of both gear and pinion surfaces should be represented in the same coordinate system, say,  $S_f(X_f, Y_f, Z_f)$ . The position vector and unit normal vector of the circular-arc curvilinear tooth gear surface can be transformed from coordinate system  $S_1(X_1, Y_1, Z_1)$  to the fixed coordinate system  $S_f(X_f, Y_f, Z_f)$  by applying homogeneous coordinate transformation matrix equations:

$$\mathbf{R}_f^{(1)} = \mathbf{M}_{fh} \mathbf{M}_{hv} \mathbf{M}_{v1} \mathbf{R}_1 \quad (7)$$

and

$$\mathbf{n}_f^{(1)} = \mathbf{L}_{fh} \mathbf{L}_{hv} \mathbf{L}_{v1} \mathbf{n}_1 \quad (8)$$

Similarly, the position vector and unit normal vector of the circular-arc curvilinear tooth pinion surface, originally represented in coordinate system  $S_2(X_2, Y_2, Z_2)$ , can be transformed to the fixed coordinate system  $S_f(X_f, Y_f, Z_f)$  by applying the following equations:

$$\mathbf{R}_f^{(2)} = \mathbf{M}_{f2} \mathbf{R}_2 \quad (9)$$

and

$$\mathbf{n}_f^{(2)} = \mathbf{L}_{f2} \mathbf{n}_2 \quad (10)$$

When the gear pair is meshed with each other, the mating tooth surfaces must satisfy the conditions of tooth continuous tangency at their instantaneous contact point as follows:

$$\mathbf{R}_f^{(1)} = \mathbf{R}_f^{(2)} \quad (11)$$

and

$$\mathbf{n}_f^{(1)} \times \mathbf{n}_f^{(2)} = 0 \quad (12)$$

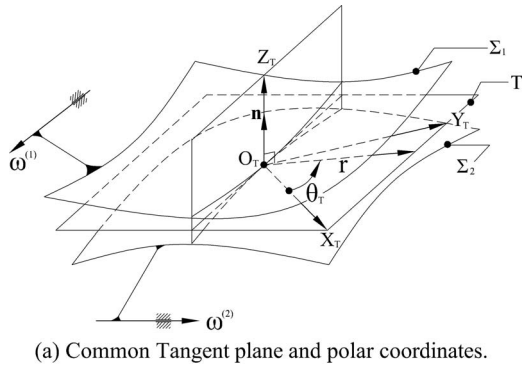
Equations (11) and (12) and two meshing equations for the gear and pinion generations form a system of seven independent equations with eight unknowns (i.e.,  $\theta^{(g)}$ ,  $\theta^{(p)}$ ,  $\gamma^{(g)}$ ,  $\gamma^{(p)}$ ,  $\phi_1$ ,  $\phi_2$ ,  $\phi_1'$  and  $\phi_2'$ ). The KE of the circular-arc curvilinear tooth gear pair can be calculated by using the following equation:

$$\text{KE} = \Delta\phi_1'(\phi_2') = \phi_1'(\phi_2') - \phi_2' \frac{T^{(p)}}{T^{(g)}} \quad (13)$$

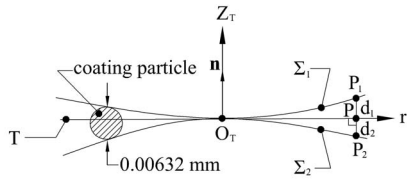
where  $T^{(g)}$  and  $T^{(p)}$  indicates the number of teeth of the gear and pinion, and  $\phi_1'(\phi_2')$  is the actual rotation angle of the gear when the gear pair is meshed under assembly errors.  $\Delta\phi_1'(\phi_2')$  is the KE of the gear set induced by the assembly errors.

**3.2 Simulation of Contact Patterns.** Owing to the elasticity of tooth surfaces, the instantaneous contact point of mating gear tooth surfaces is spread over an elliptical area. The location of geometric center of the instantaneous contact ellipse coincides with the theoretical contact point, which is obtained by TCA. The bearing contact of the gear drive is formed as a set of contact ellipses. Usually, the contact pattern can be measured on a gear pattern testing machine. The gear tooth surface is smeared with a coating, and the diameter of the coating is  $6.32 \mu\text{m}$ .

Actually, the contact pattern can also be obtained by applying the surface topology method and numerical simulation method. Figure 6(a) displays the relationship among two contact tooth surfaces and their common tangent plane, where point  $O_T$  is the instantaneous contact point of two mating gear tooth surfaces  $\Sigma_1$



(a) Common Tangent plane and polar coordinates.



(b) Measurements on surface separation distance.

**Fig. 6 Simulation of a contact ellipse (a) common tangent plane and polar coordinates; (b) measurements on surface-separation distance**

and  $\Sigma_2$ . Vector  $\mathbf{n}$  is the common unit normal vector of these two mating tooth surfaces, and  $T$  indicates the common tangent plane to the mating tooth surfaces. The perpendicular distances measured from point  $P$ , on the tangent plane  $T$ , to the mating tooth surfaces  $\Sigma_1$  and  $\Sigma_2$  are designated as  $d_1$  and  $d_2$ , as illustrated in Fig. 6(b). Thus, the total separation distance of these two mating tooth surfaces at point  $P$  can be expressed as  $d=d_1+d_2$ , where  $d_1+d_2$  is equal to  $|Z_T^{(1)}-Z_T^{(2)}|$ , and  $Z_T^{(1)}$  and  $Z_T^{(2)}$  represent the coordinates of points  $P_1$  and  $P_2$  of the  $Z_T$  component, respectively. An auxiliary polar coordinate system  $(r, \theta_T)$  is defined and parameter  $r$  represents the distance measured outward from the contact point  $O_T$  to the searched separation point  $P$ , as shown in Fig. 6, and  $\theta_T$  indicates the angular position with the range of  $\theta_T$  beginning from 0 to  $2\pi$ . All the equal separation-distance points of two mating tooth surfaces can be calculated by solving the following system of equations:

$$X_T^{(1)} = X_T^{(2)} \quad (14)$$

$$Y_T^{(1)} = Y_T^{(2)} \quad (15)$$

$$\tan(\theta_T) = \frac{Y_T^{(1)}}{X_T^{(1)}} \quad (16)$$

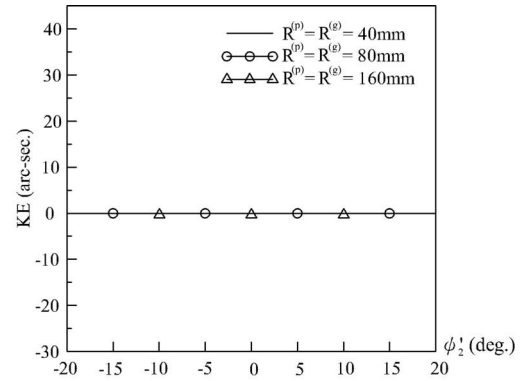
and

$$|Z_T^{(1)} - Z_T^{(2)}| = 6.32 \mu\text{m} \quad (17)$$

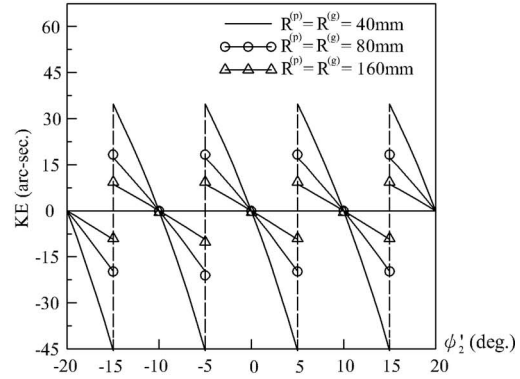
Therefore, the unknown parameters can be solved by applying Eqs. (14)–(17) with a numerical method. Based on the above-

**Table 1 Major design parameters for the curvilinear tooth gear set**

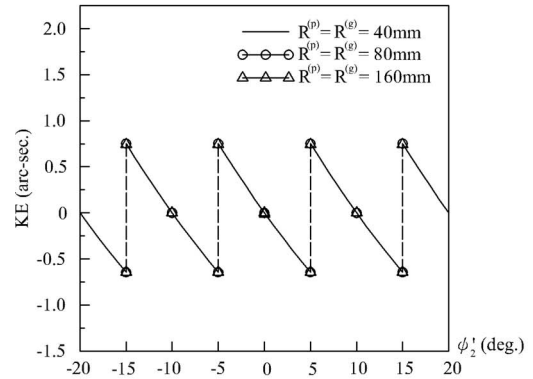
Design parameters	Pinion	Gear
Number of teeth ( $T^{(i)}$ )	18	36
Normal module ( $M$ )	3 mm/tooth	3 mm/tooth
Normal pressure angle ( $\alpha$ )		20 deg
Radius of the curvilinear tooth-trace ( $R_{ab}$ )		30 mm
Face width ( $W$ )		30 mm



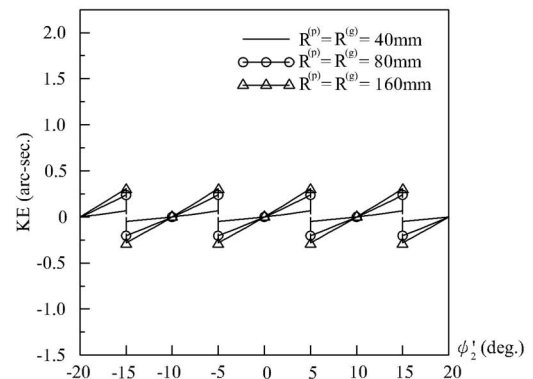
(a) Ideal Assembly Condition



(b)  $\Delta C = 0.1\text{mm}$



(c)  $\Delta\gamma_h = 0.1\text{deg}$ .



(d)  $\Delta\gamma_v = 0.1\text{deg}$ .

**Fig. 7 Kinematical errors of the gear pair with different  $R^{(i)}$  under different assembly conditions ( $R_{ab}=30\text{mm}$ )**



**Table 2 Contact ratios under different design parameters**

Design parameters: $M=3$ mm/tooth, $A=1M$ , $B=1M$ , $T^{(g)}=36$ teeth, $T^{(p)}=18$ teeth						
$R_{ab}$ (Figs. 1 and 4) (mm)	$R^{(g)}$ (Fig. 3) (mm)	$R^{(p)}$ (Fig. 3) (mm)	$\alpha$ (Fig. 3) (deg)	$\phi_{1b}$ (deg)	$\phi_{1e}$ (deg)	CR
30	80	80	20	-13.54	5.45	1.90
30	80	80	25	-11.53	4.60	1.61
30	40	40	20	-15.03	4.99	2.00
20	80	80	20	-13.54	5.45	1.90

$\phi_{1b}$  represents the rotation angle of the gear at the beginning point of contact and  $\phi_{1e}$  represents the rotation angle of the gear at the end point of contact.

mentioned algorithm, a computer program is developed to determine the points, which the amount of surface-separation distance is the same as the thickness of the coating for contact pattern tests.

#### 4 Numerical Examples for Meshing Simulations of Gear Drives

*Example 1.* The relationships between the KE and radius  $R^{(i)}$  (Fig. 3) of the circular-arc cutter profile are investigated. Some major design parameters of the circular-arc curvilinear tooth gear pair are shown in Table 1. This example investigates the gear pair meshing under different  $R^{(i)}$ , and it is defined that  $R^{(g)}=R^{(p)}$  for two complemented circular-arc rack cutters.

The KE curves of the mating gear pair meshing under different assembly conditions are shown in Fig. 7. It is found that this type of gear pair is very sensitive to the center distance variation, and KE is decreased with the increase in  $R^{(i)}$  when the center distance assembly error  $\Delta C=0.1$  mm. It is known that gears with involute tooth profiles induce no KE with center distance assembly errors. It means that when  $R^{(i)}$  approaches to infinity then the gear pair becomes the involute profile and KE becomes zero (Fig. 7(b)). However, if the gear pair has an axial misalignment  $\Delta\gamma_v=0.1$  deg, then the KE increases with the increase of  $R^{(i)}$ . According to Figs. 7(c) and 7(d), this type of gears allow gear axial misalignments.

*Example 2.* In this example, contact ratios of the gear pair are studied. The contact ratio of a gear set is defined as the average number of teeth in contact during the gear meshing. Therefore, the contact ratio can be calculated by the gear's rotation angle, measured from the beginning point of contact to the end point of contact, divided by the angle formed by two successive teeth (i.e.,  $360 \text{ deg}/T^{(g)}$ ). Herein,  $T^{(g)}$  is the numbers of gear teeth. Thus, the contact ratio (CR) can be obtained from the result of TCA and expressed by the following equation:

$$CR = T^{(g)} \left( \frac{\phi_{1e} - \phi_{1b}}{360 \text{ deg}} \right) \quad (18)$$

where angles  $\phi_{1e}$  and  $\phi_{1b}$  represent the end point of contact and the beginning point of contact of the gear rotation angle, respectively. These two angles can be determined based on the TCA simulation results. Therefore,  $\phi_{1e} - \phi_{1b}$  denotes the rotation angle of the gear while one pair of gear teeth is in mesh within the range of gear tooth surface.

In this example, the major design parameters of the gear pair are the same as those listed in Table 1. Table 2 illustrates the contact ratios versus different major design parameters of the gear set. Contact ratio increases with the decrease of the pressure angle and radius of the cutter's circular-arc profiles. However, the radius  $R_{ab}$  of the face-mill cutter (i.e. radius of curvilinear tooth-trace) takes no effect on the contact ratio.

*Example 3.* A value of  $\Delta R$  is pre-designed in this example, and  $\Delta R$  is defined as  $\Delta R=(R^{(p)}-R^{(g)})$ . The major design parameters of

the circular-arc curvilinear tooth gear set are the same as those shown in Table 1.

KEs under different meshing conditions with different  $\Delta R$  are illustrated in Fig. 8, where  $\Delta R=0, 2,$  and  $4$  mm. There is no KE under ideal assembly conditions with  $\Delta R=0$  mm because the gear pair is generated by two complemented rack cutters. However, the gear pair with  $\Delta R \neq 0$  possesses a parabolic type of KE curve under the ideal assembly condition. Relationships between KE and  $\Delta R$  under different meshing conditions are shown in this figure. It is found that center distance error  $\Delta C$  has a significant influence on the KE of the gear pair since the proposed gear drive has circular-arc tooth profiles.

*Example 4.* Let us investigate the KEs of the gear pair with different radii  $R_{ab}$  of the curvilinear tooth-trace (Fig. 4) under different assembly conditions. The design parameters of the gear pair are the same as those shown in Table 1 with  $R^{(g)}=R^{(p)}=80$  mm. The KE curves of the gear pair under different meshing conditions are shown in Fig. 9.

The gear pair generated by two complemented rack cutters has no KE meshing under ideal assembly conditions. It is found that KE caused by the center distance assembly error is quite severe but it is not sensitive to the value of  $R_{ab}$ . It is due to the fact that the circular-arc curvilinear tooth gear pair is in point contacts, and the contact point of the gear pair is located on the cross section of  $Z^{(i)}=0$  mm (i.e.  $\gamma^{(i)}=0$  deg shown in Fig. 4) under the ideal assembly condition and with center distance error. Therefore, the KE indeed depends on the circular-arc tooth profile of the gear pair and has no relationship with the radius of curvilinear tooth-trace of the gear pair. It is also found that KE is decreased with the decrease of  $R_{ab}$  under a horizontal misaligned angle  $\Delta\gamma_h$ . It means that a larger curvature (i.e., a smaller  $R_{ab}$ ) of the curvilinear tooth-trace allows a larger tolerance to the horizontal axial misalignment of the gear pair. However, KE is increased with the decrease of  $R_{ab}$  under a vertical misaligned angle  $\Delta\gamma_v$ . Therefore, a circular-arc curvilinear tooth gear pair is very sensitive to the center distance assembly error. However, the axial misalignments and  $R_{ab}$  are not sensitive to the KE of the gear pair.

*Example 5.* The contact patterns under different assembly conditions are acquired by the developed TCA computer simulation programs. The bearing contacts are localized near the middle region of the tooth flank due to the curvilinear tooth-trace of the gear pair. The major design parameters of the gear pair are the same as those listed in Table 1 except that  $R^{(g)}=R^{(p)}=40$  mm with different values of curvilinear tooth-trace  $R_{ab}$ .

Figure 10 shows the contact ellipses that appeared on the gear tooth surfaces of the gear pair with  $R_{ab}=20, 30,$  and  $40$  mm, respectively, under ideal assembly condition. In Fig. 10, symbol  $\phi'_1=\phi_{1b}$  indicates the rotation angle of the gear at the beginning point of contact while  $\phi'_1=\phi_{1e}$  represents the rotation angle of the gear at the end point of contact.  $\phi_{1b}$  and  $\phi_{1e}$  are obtained from TCA results and shown in Table 2. Meanwhile, the contact ratio of the gear drive can be calculated by applying Eq. (18). The contact

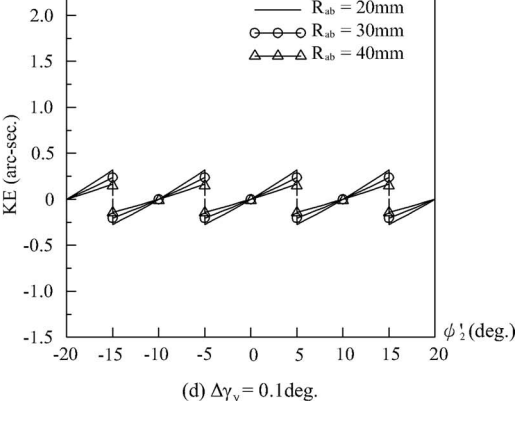
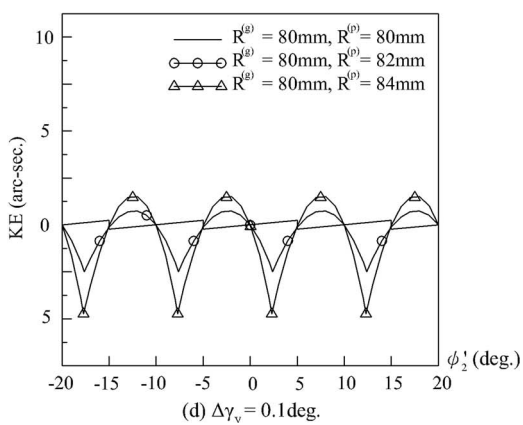
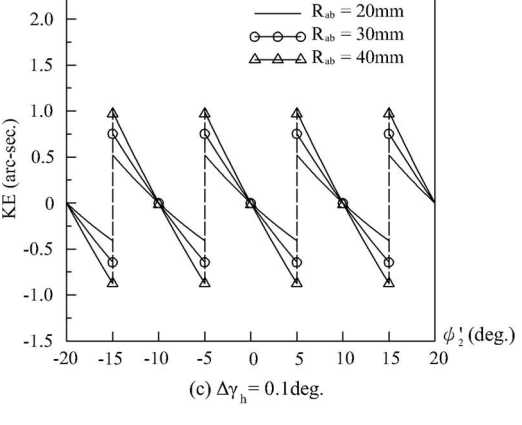
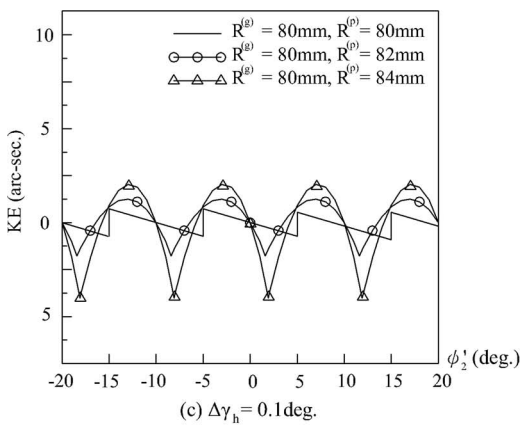
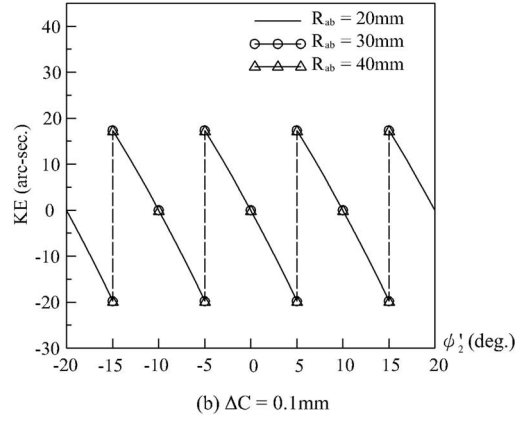
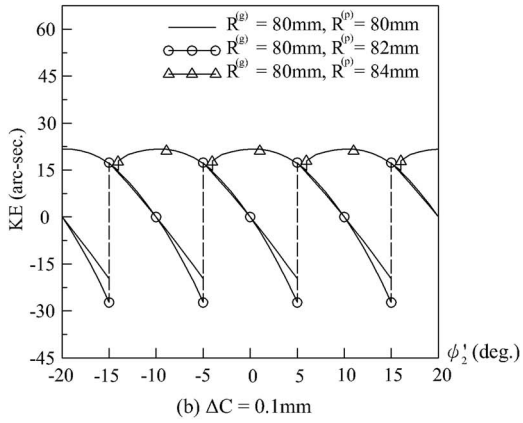
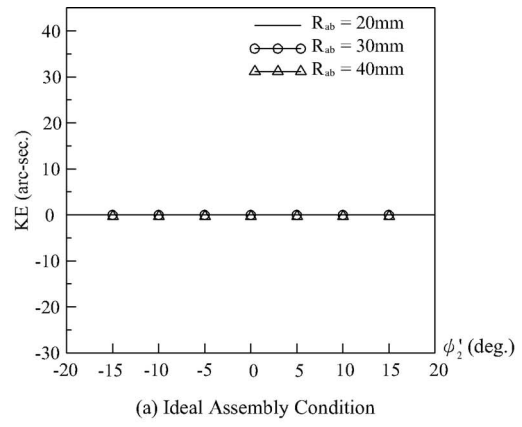
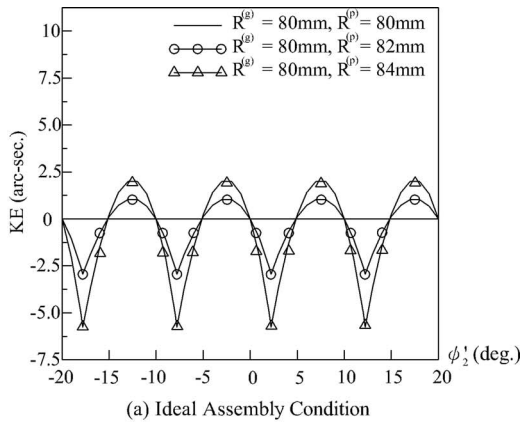
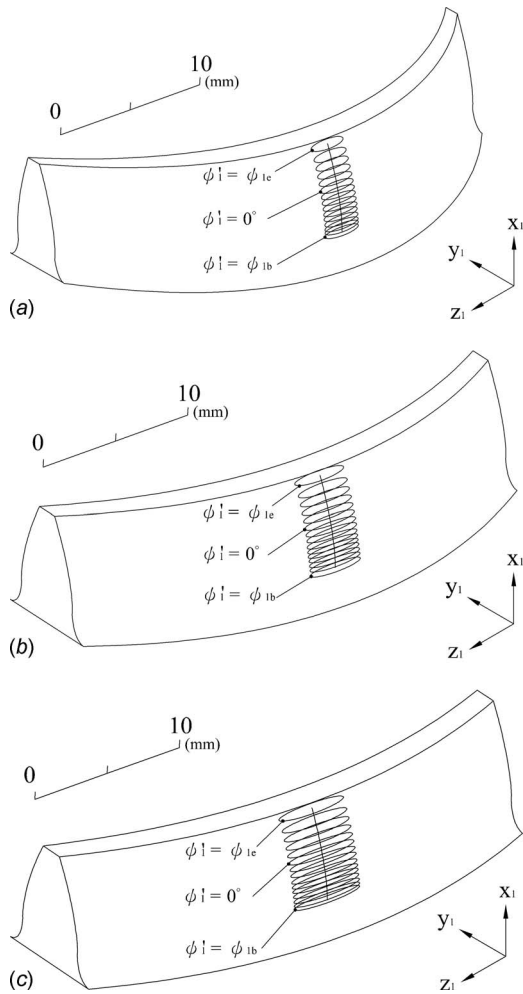


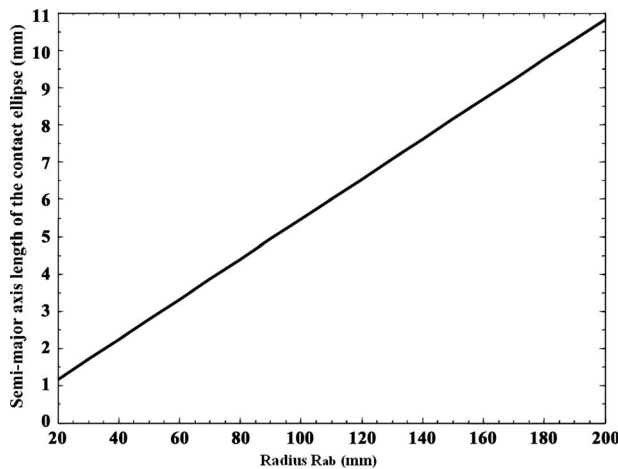
Fig. 8 Kinematical errors of the gear pair with different  $\Delta R$  under different assembly conditions ( $R_{ab}=30\text{ mm}$ )

Fig. 9 Kinematical errors of the gear pair with different  $R_{ab}$  under different assembly conditions ( $R^{(p)}=R^{(g)}=80\text{ mm}$ )



**Fig. 10** Contact ellipses on the gear tooth surfaces under ideal assembly condition with different values of  $R_{ab}$ : (a)  $R_{ab} = 20$  mm ( $R^{(g)} = R^{(p)} = 40$  mm); (b)  $R_{ab} = 30$  mm ( $R^{(g)} = R^{(p)} = 40$  mm); (c)  $R_{ab} = 40$  mm ( $R^{(g)} = R^{(p)} = 40$  mm)

points of the gear pair are all located at the middle region of the gear flank no matter  $R_{ab} = 20, 30,$  or  $40$  mm, and the length of the major axis of contact ellipses increases evidently with the increase of  $R_{ab}$ . This is due to the fact that a larger radius of  $R_{ab}$  induces a smaller crowning effect on the tooth flank. If the radius  $R_{ab}$  tends



**Fig. 11** Relationship of design parameter  $R_{ab}$  versus the semi-major axis length of the contact ellipse

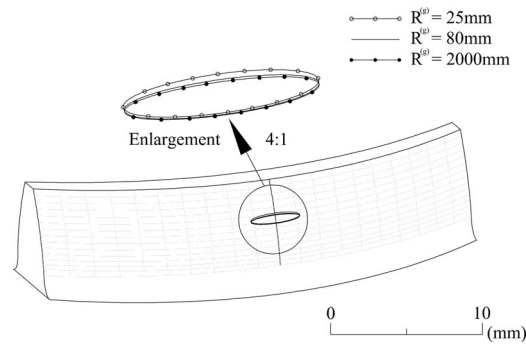


**Fig. 12** Contact ellipses on the gear tooth surface with different  $R^{(i)}$

to infinity, the curvilinear tooth gear becomes a spur gear. Figure 11 shows the effects of design parameter  $R_{ab}$  on the semi-major axis length of the contact ellipse. It is found that the semi-major axis length is proportional to  $R_{ab}$ .

*Example 6.* One of the main advantage of the circular-arc curvilinear tooth gear drive is to reduce the contact stress efficiently by increasing the area of contact ellipses on the contact tooth surfaces. Therefore, contact ellipse is the key index to predict the contact situation. The area of the contact ellipse depends on the lengths of major and minor axes of the contact ellipse. In this example, the gear parameter  $R^{(i)}$  is chosen to investigate the effects on the corresponding semi-minor axis of the contact ellipse, while the radius of the curvilinear tooth-trace is fixed as  $R_{ab} = 30$  mm (Figs. 1 and 4). Major design parameters for this example are chosen the same as those listed in Table 1. It is noted that the radii of circular-arc tooth profiles  $R^{(g)} = R^{(p)}$  for two complemented rack cutters, as shown in Figs. 2 and 3, are chosen as 25 mm, 80 mm and 2000 mm herein.

Figure 12 shows the length of minor-axis of the contact ellipse and it is inverse proportional to the radius  $R^{(i)}$ . Figure 13 shows the relationships between the design parameter  $R^{(i)}$  to the length of semi-major axis and semi-minor axis of the contact ellipse under ideal assembly condition. It is noted that the length of the semi-minor axis of the contact ellipse can be increased significantly by designing of a gear drive with a smaller value of  $R^{(g)}$ , but variation of  $R^{(g)}$  almost has no effect on the length of semi-major axis of contact ellipse. However, as stated in Example 5, the length of semi-major axis can be increased by the increase in radii  $R_{ab}$  of the curvilinear tooth-trace, as shown in Fig. 11.

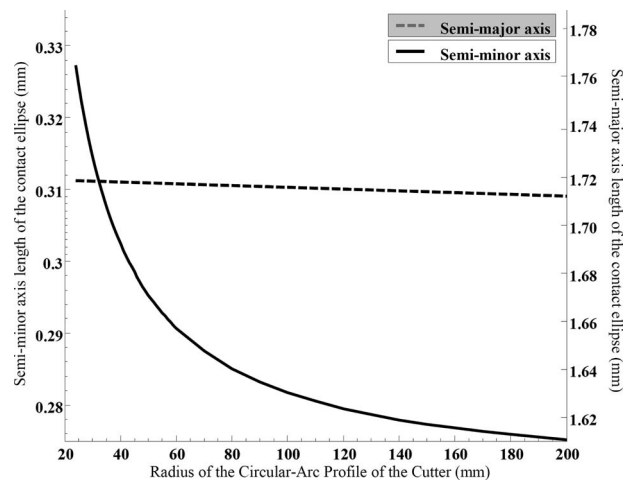


**Fig. 13** Relationship of design parameter  $R^{(i)}$  versus the semi-major and semi-minor axis lengths of the contact ellipse

## 5 Conclusions

In this study, two complemented rack cutters are designed as curvilinear tooth-traces with their normal sections of circular-arc tooth profiles for generation of the proposed circular-arc curvilinear tooth gear drives. Mathematical model of this type of gears has been derived based on the theory of gearing and gear generation mechanism. The advantages of the proposed gear drive are having a higher load carrying capacity, without axial thrust force and not sensitive to axial assembly misalignments.

The TCA computer simulation programs have been developed for the proposed circular-arc curvilinear tooth gear drive. The effects of the gear design parameters and assembly errors on the contact ellipse, contact ratio and KE of the mating gear drive can be predicted by the computer simulations. The resultant KE curve of the gear drive can be modified into a parabolic type by appropriately choosing the design parameter  $\Delta R$ .

The effects of the assembly errors and major gear design parameters on the shape of contact ellipses are acquired by applying the developed TCA computer simulation programs and surface topology method. The area of the contact ellipse can be adjusted by changing the radius  $R_{ab}$  of the curvilinear tooth-trace and the radius  $R^{(i)}$  of circular-arc tooth profile of the cutter. The length of the major-axis of contact ellipses is directly proportional to the radius  $R_{ab}$  of the curvilinear tooth-trace. Meanwhile, the minor-axis of contact ellipses is inverse proportional to the radius  $R^{(i)}$  of

the circular-arc tooth profile. By properly choosing a smaller value of circular-arc tooth radius  $R^{(i)}$  and a larger curvilinear tooth radius  $R_{ab}$  of the circular-arc curvilinear tooth gear drive, the area of its contact ellipses can be increased significantly.

## Acknowledgment

The authors would like to thank to the National Science Council of R.O.C. for supporting of this research under the Grant No. NSC 94-2212-E-009-009.

## References

- [1] Liu, S. T., 1988, "Curvilinear Cylindrical Gears," *Gear Technol.*, **5**, pp. 8–12.
- [2] Tseng, R. T., and Tsay, C. B., 2001, "Mathematical Model and Undercutting of Cylindrical Gears with Curvilinear Shaped Teeth," *Mech. Mach. Theory*, **36**, pp. 1189–1202.
- [3] Tseng, J. T., and Tsay, C. B., 2006, "Undercutting and Contact Characteristics of Cylindrical Gears With Curvilinear Shaped Teeth Generated by Hobbing," *ASME J. Mech. Des.*, **128**, pp. 634–643.
- [4] Wildhaber, E., 1926, "Helical Gearing" U.S. Patent, No. 1,601,750.
- [5] Novikov, M. L., 1956, USSR Patent No. 109,750.
- [6] Litvin, F. L., and Tsay, C. B., 1985, "Helical Gears With Circular Arc Teeth: Simulation of Conditions of Meshing and Bearing Contact," *ASME J. Mech., Transm., Autom. Des.*, **107**, pp. 556–564.
- [7] Litvin, F. L., and Fuentes, A., 2004, *Gear Geometry and Applied Theory*, Cambridge University Press, Cambridge.
- [8] Litvin, F. L., 1989, "Theory of Gearing," NASA Reference Publication No. RP-1212.
- [9] Janninck, W. K., 1988, "Contact Surface Topology of Worm Gear Teeth," *Gear Technol.*, **5**(2), pp. 31–47.